

Cleaner Energy Storage: Cradle-to-Gate Lifecycle Assessment of Aluminium-ion Batteries with an Aqueous Electrolyte

N. Melzack*, R. G. A. Wills, A.J Cruden
Energy Technology Group, University of Southampton, UK

Abstract

In the context of growing demand on energy storage, exploring the holistic sustainability of technologies is key to future-proofing our development. In this paper, a cradle-to-gate Lifecycle assessment of aqueous electrolyte aluminium-ion (Al-ion) batteries has been performed. Due to their reported characteristics of high power (circa 30 W kg⁻¹ active material) and low energy density (circa 15 Wh kg⁻¹ active material), these results were compared with supercapacitors (per kW). Initial findings suggest these aluminium-ion cells have fewer environmental impacts than commercial supercapacitors, hence offer a more environmentally sensitive energy storage technology solution. Al-ion batteries are in their early development, and this result shows a strong argument for continuing research into this technology alongside other emerging energy storage systems.

Keywords: Aluminium-ion batteries, Life cycle (impact) assessment, aqueous electrolyte, energy storage (batteries), environmental impact assessment

Corresponding author: N. Melzack

n.melzack@soton.ac.uk

1. Introduction

In the search for sustainable energy there is a diverse range of renewable methods to generate electricity such as wind and solar. Of course, the question then arises on the use of this energy, and how it is stored when not needed. Looking into sustainable energy storage (such as supercapacitors and batteries) is therefore critical for a fully sustainable energy service. This is true both for grid storage and the smaller storage devices in our cars and phones.

Al-ion (aluminium ion) batteries have received recent interest as alternatives to Li-ion (lithium-ion) chemistries (Elia, et al., 2021). While there are aqueous Li-ion technologies (Profili, et al., 2020), most studies have looked at ionic liquid electrolytes and preliminary environmental comparisons have been made (Ellingsen, et al., 2018, Salgado Delgado, 2019). Utilising an aqueous electrolyte may have life cycle assessment (LCA) benefits compared to organic and ionic liquid systems. The potential ionic storage of aqueous electrolytes is two orders of magnitude higher than that of organic non-aqueous electrolytes – this could enable far higher power capability as well (Zhang, et al., 2020). The aqueous electrolyte Al-ion cell (Holland, et al., 2018) is a good candidate for analysis as its performance characteristics overlap with both supercapacitor and battery application areas. It is also a new chemistry and offers the opportunity to develop the system in synergy with LCA, rather than undertaking a LCA as a retrospective assessment. Its high-power density (300 W kg⁻¹ (Holland, et al., 2018)) and energy density (15 Wh kg⁻¹ (Holland, et al., 2018)) show promise for the development of a commercial, useable product. The Al-ion cell consists of a titanium dioxide (TiO₂) negative electrode and a copper hexacyanoferrate (CuHCF) positive electrode, and has reported cycle life of 1750 cycles at 20 C. However with 7% capacity fade after these cycles – there is potential for a longer cycle life and 1750 may have been a limit of the study – not the cell (Holland, et al.,

2018). Performing an LCA on this Al-ion cell is therefore a useful tool in understanding the sustainability of the cell itself, in terms of its material constituent parts. Due to the high-power density of the cell, and observations of self-discharge, this cell behaves similarly to a supercapacitor, and is seen as a potential hybrid cell, and is compared to LCAs of supercapacitors in section 3.2.

There is little literature on supercapacitor LCAs, however a hybrid battery-supercapacitor has been assessed in the past - (Conte, et al., 2014) and found fewer environmental impacts than traditional supercapacitors. A more recent supercapacitor LCA (Cossutta, et al., 2020) looked at two electrode materials activated carbon and graphene – finding overall an activated carbon electrode had fewer environmental impacts. No LCAs of aqueous supercapacitors could be found. The results of (Cossutta, et al., 2020) is compared to this work in terms of the environmental impact to understand the key differences and to also see where potential improvements can be made if scaled up.

2. Methodology

This LCA looked at the cradle-to-gate section of the product lifecycle, using the methodology set out in (Siret, 2018, Potocnik, 2013). Cradle-to-gate includes the mining and production of raw materials through to manufacture, but does not include the use phase, or any second-life applications or end of life activities (such as recycling).

Then, using the information available from Holland (Holland, et al., 2018, Holland, 2018) and The University of Southampton, the raw materials that formed each component were listed. The mass of each raw material used was then calculated based on the electrode masses given by to construct the cell described. Using OpenLCA v 1.10.3 (Ciroth, 2007) software, the processes and emissions involved in obtaining the raw materials were backed with either the ecoinvent 3.2 database (Steubing, et al., 2016), or the Gabi Think Step database (AG Thinkstep, 2012) – as used in (Siret, 2018). The distance from key production locations to the UK was calculated. Production of the overall cell was then scaled to provide the correct mass for 1 functional unit (FU), and the impact assessment was performed.

The environmental impact across 19 categories were then assessed per FU using the European Union's Environmental Footprint (EUEF) methods (Potocnik, 2013). The outputs were analysed and compared to similar LCAs for other battery technology to understand where the Al-ion technology sits with its potential peers. To allow for comparison with other technology, the energy used in production was scaled from information provided in (Siret, 2018), however this was not directly calculated for the Al-ion cell. The process used in this paper followed that shown in Figure 1, from detailing the cell components through to analysis of the full cell.

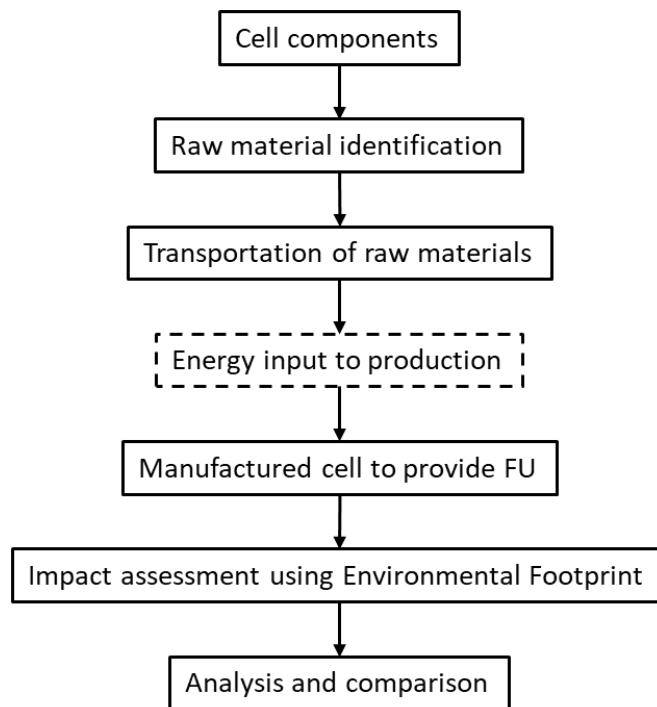


Figure 1 LCA process

2.1. Raw material identification

The cell components were first identified as:

- the positive electrode, which comprised a carbon-polymer substrate onto which an active layer was coated. The active layer contained copper hexacyanoferrate, CuHCF, (active material), carbon black to improve electrical conduction and Nafion as an electrolyte/ion permeable binder.
- negative electrode, which comprised a carbon-polymer substrate onto which an active layer was coated. The active layer contained TiO₂ (active material), carbon black to improve electrical conduction and Nafion as an electrolyte/ion permeable binder.
- current collectors, which were copper foil, placed on the outer (non-electrolyte) face of the carbon-polymer substrate.
- electrolyte, which comprised an aqueous solution of KCl and AlCl₃.
- cell chamber, which comprised a PEEK (polyether ether ketone) gasket to separate the electrodes and provide a reservoir for the electrolyte.
- battery casing, which comprised PEEK.

The cell manufacturing process was taken from the literature (Holland, et al., 2018) and shown in Figure 2. The active materials for the positive and negative electrode active layers were mixed into inks, which were then coated onto the carbon-polymer substrates and cut to shape to form the electrodes. The components were assembled and clamped together with the PEEK casing. A cross-sectional diagram of the resulting cell is provided in Figure 3, which shows the PEEK cell casing on each outer face, inside which is the copper current collector and carbon-polymer substrate. The positive and negative active materials layers are shown on the left and right carbon-polymer

substrate respectively and between the two electrodes is the electrolyte reservoir. The PEEK gasket forming the cell chamber and holding the electrolyte reservoir is not shown. A full material inventory can be found in S1.

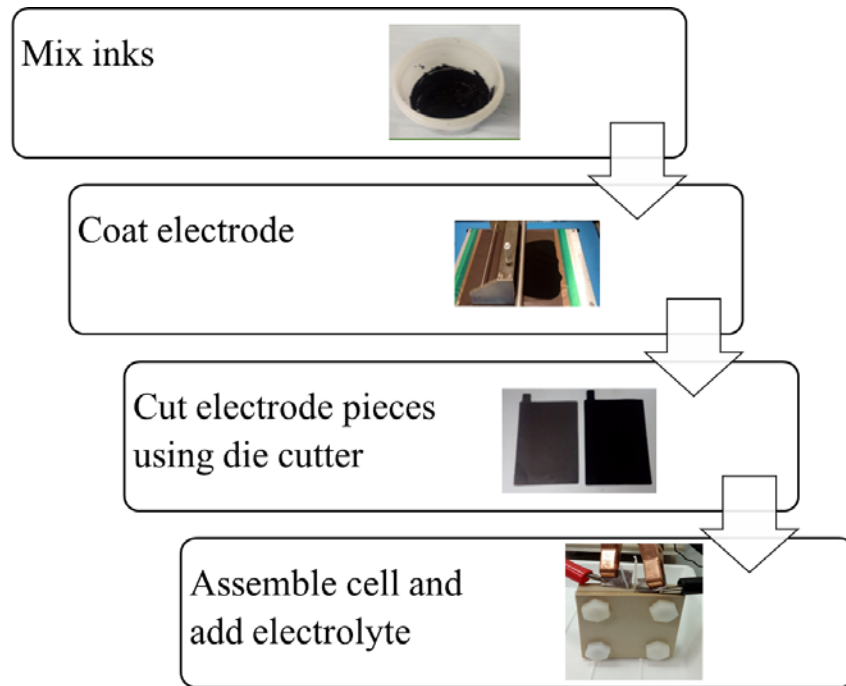


Figure 2 Cell construction process (Holland, et al., 2018)

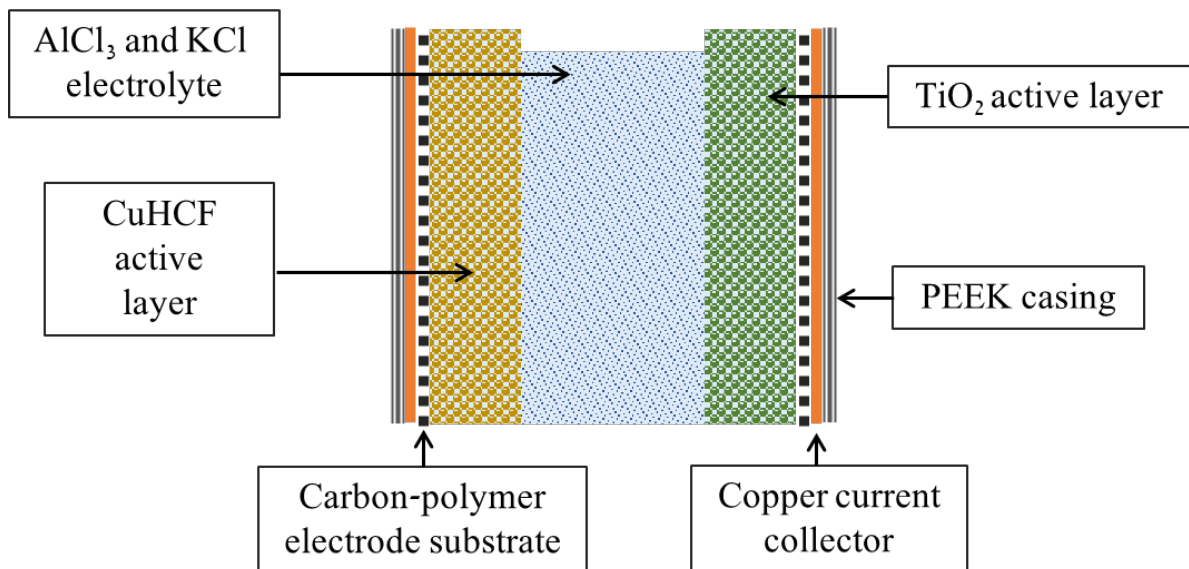


Figure 3 Cross section of the assembled cell

2.1.1. Electrodes

For each electrode, a mixture of active material, carbon black, and Nafion binder was prepared – a dry mix. Isopropanol was then added to these mixes to create an electrode ink which was applied to a Sigracell PV10 carbon polymer electrode substrate from SGL carbon (SGL Carbon, 2021). The materials common to both electrodes are discussed first, followed by the active materials and ratios of mixtures for the individual electrodes. The processes involved in the production of carbon black has been taken from the ecoinvent 3.2 database. With regards to Nafion, as this is a branded product, the constituent parts have been taken from (Mauritz and Moore, 2004) and therefore an estimate for production processes and proportions were made, with the inputs taken from the ecoinvent 3.2 database. See S1 for full breakdown of these parts. Isopropanol has a well-defined production method, and the processes involved in producing isopropanol were taken from the ecoinvent 3.2 database. Like Nafion, the Sigracell PV10 electrode substrate is a branded product and as such the constituent parts and proportions have been assumed based on (Sigracell, 2016) and general carbon polymers, including polyvinyl fluoride and polycarbonate– the processes of which were taken from the GaBi Thinkstep database (AG Thinkstep, 2012). The active material for the positive electrode was copper hexacyanoferrate (CuHCF), and anatase TiO₂ nanopowder for the negative electrode.

2.1.2. Positive active material (CuHCF)

The steps used to make the positive electrode (Holland, et al., 2018) are:

1. CuHCF was made using a mixture of 1.5 mol dm⁻³ solution Cu(NO₃)₂ and 1 mol dm⁻³ solution of K₃[Fe(CN)₆]. The processes involved in the production of both Cu(NO₃)₂ and K₃[Fe(CN)₆] are taken from the ecoinvent 3.2 database.
2. CuHCF, carbon black, and a Nafion binder were mixed in the ratio 8:1:1 by wt% to create a dry mix
3. Isopropanol was then added to form inks in the proportions of approximately 3:1 (isopropanol:active material).
4. The ink was then painted on Sigracell PV10 carbon polymer electrode substrate from SGL.

The total weight of the electrode ink layer was 38mg, and the Sigracell PV10 substrate weighs ~10g (Sigracell, 2016). Figure 4 shows the production flow from the positive electrode to its constituent parts to the positive electrode. The positive electrode materials comprise the carbon-polymer substrate and CuHCF ink. The electrode substrate further comprises polycarbonate and polyvinyl fluoride, while the CuHCF ink comprises seven materials: isopropanol, copper nitrate, potassium ferrocyanide, alcohol ether sulphate chlorine dioxide, hydrogen fluoride and tetrafluoroethane. Details on specific masses, processes, and datasets used for these raw materials can be found in S1. The packaging and transport has been taken into account for the items shown – a plastic packaging or glass bottle is assumed based on the item. The packaging processes are taken from the ecoinvent 3.2 database.

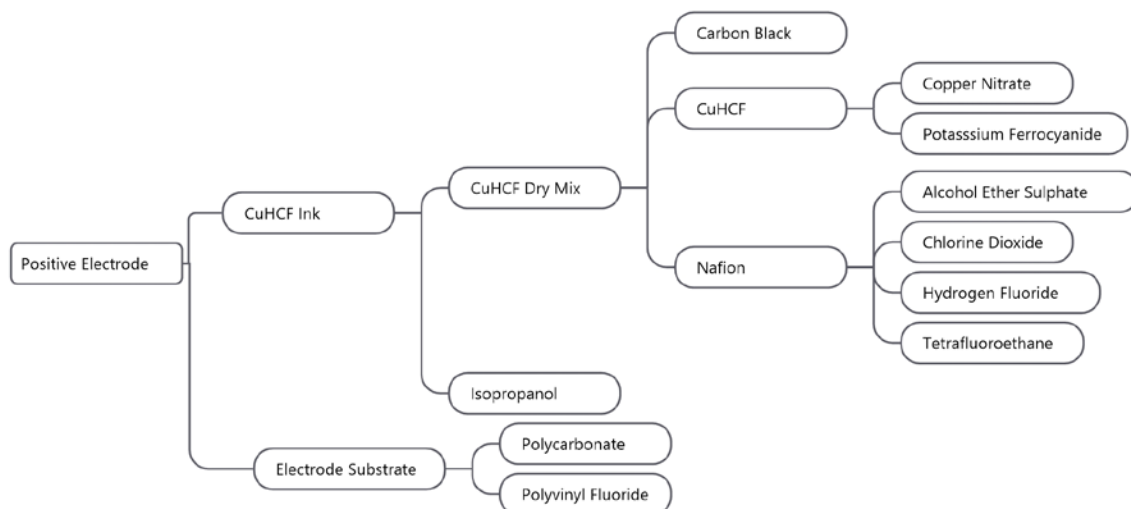


Figure 4 Production flow for the positive electrode redrawn from the ecoinvent 3.2 database output.

2.1.3. Negative active material (TiO₂)

The steps used in making the negative electrode are:

1. TiO₂ commercial nano-powder from Sigma Aldrich, carbon black, and a Nafion binder were mixed in the proportion 9:0.5:0.5 by wt% to create a dry mix. Standard TiO₂ was assumed as the base of the nano-powder, with the processes involved in the mining and production taken from the ecoinvent 3.2 database.
2. Isopropanol was then added to form inks in the proportions of approximately 3:1 (isopropanol:active material)
3. The ink was then painted on Sigracell PV10 carbon polymer current collectors from SGL.

The total weight of the dry ink layer was 85 mg. As with the positive electrode, Figure 5 shows the production flow for the materials of the negative electrode. The negative electrode materials comprise the carbon-polymer substrate and TiO₂ ink. The electrode substrate further comprises polycarbonate and polyvinyl fluoride, while the TiO₂ ink comprises seven materials: isopropanol, TiO₂, alcohol ether sulphate chlorine dioxide, hydrogen fluoride and tetrafluoroethene. Details on specific masses, processes, and datasets used for these raw materials can be found in S1.

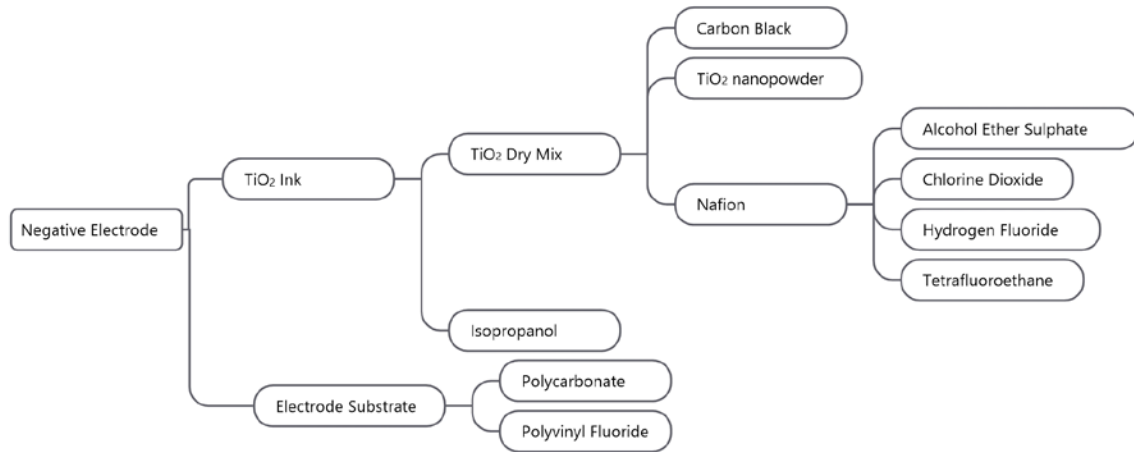


Figure 5 Production flow for negative electrode redrawn from OpenLCA

2.1.4. Electrolyte components

The electrolyte used was 1 M AlCl_3 and 1 M KCl in de-ionised water. The processes involved in the production of these chemicals have been taken from the ecoinvent 3.2 database. It is assumed that a total of 6 g of electrolyte was used, given the spacing in the electrolyte cavity (Holland, 2018), this value will be investigated further in future cell-builds. Figure 6 shows the production flow for the electrolyte.

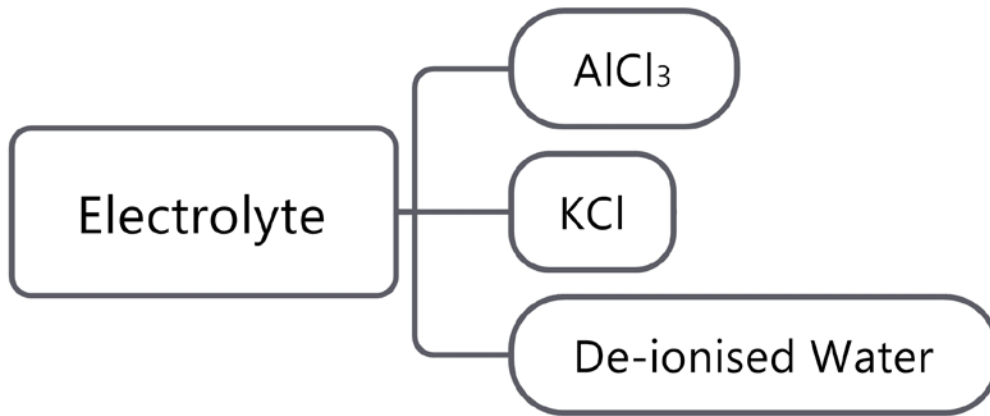


Figure 6 Production flow for electrolyte redrawn from OpenLCA

2.1.5. Battery casing and other supporting materials

The current collectors are copper sheets, given the 10 × 10 cm layout of the electrode (Holland, 2018), and typical values for copper current collectors (Choi, et al., 2013) 1 g is assumed for each current collector. This value will be investigated further in future cell-builds. The processes involved in the production of copper sheets have been taken from the ecoinvent 3.2 database. The battery casing is assumed to be a thermosetting plastic (processes for production taken from the GaBi Thinkstep database), and that 2.5 g would be appropriate for a cell of this size. The overall construction of an Al-ion cell will be similar to a Pb-acid, which have varying casing contributions around 10% (Ballantyne, et al., 2018, Liu, et al., 2015), with other Li-ion cases being between 8% and 24% of the total mass (Siret, 2018, Peters and Weil, 2018, Kim, et al., 2016).

The full cell therefore is made up of both electrodes, current collectors, the electrolyte and the battery casing. A summary of the percentage by weight of each component is presented in Figure 7. The positive electrode, negative electrode and electrolyte each contribute slightly over one quarter of the overall mass (27%), with the casing and current collector combined making up the remaining 20%. Transportation of raw materials

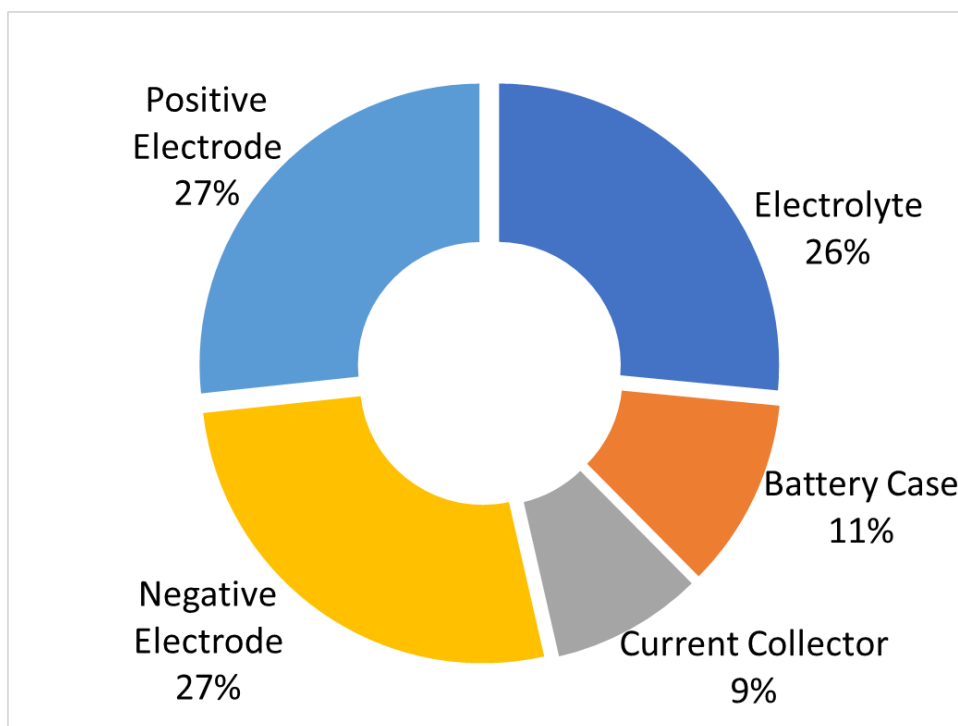


Figure 7 Cell component breakdown by % wt

2.2. Transportation of raw materials

Transportation of raw materials have been considered from the point of mining/processing/production to delivery to the UK. Countries of high production were based on the US Geological Survey (U.S. Geological Survey, 2020). A summary of the main components for the aqueous Al-ion cell are presented in Table 1. Their geographical source area is identified along with the approximate distance for transporting the component to a manufacturing plant in the centre of Great Britain. Potash shown in the table, for the production of KCl and potassium ferricyanide, are not shown in Figures 4 or 5, as the datasets which comprise manufacture of these materials (from ecoinvent 3.2) already take this into account. However to understand the transport distances of such items, potash was considered. This is similar for aluminium, as $AlCl_3$ production from the dataset already considers the aluminium component. The transport is not shown in Figures 4, 5 and 6.

Table 1 Geographical location of production and associated delivery distance to the UK for key components of the aqueous Al-ion cell.

Material	Global Area (U.S. Geological Survey, 2020)	Distance (km)
Potash (for KCl and Potassium ferricyanide)	Canada	6000 (Siret, 2018)
Copper (for current collector and Copper Nitrite)	Chile	11900 (Siret, 2018)
Titanium dioxide	China	8000 (Siret, 2018)
Aluminium (for $AlCl_3$ production)	China	8000(Siret, 2018)

Carbon/hydrocarbons (for carbon black and plastics)	Europe Mainland	1000 (Siret, 2018)
Nafion (used in electrode ink)	Europe Mainland	1000 (Siret, 2018)
Isopropanol (used in electrode ink)	Within UK	500*

*based on Sigma Aldrich order data, assuming manufacture in centre of Great Britain (Leeds) and a non-direct route due to delivery service

2.3. Functional unit identification

The functional unit is a reference unit which normalises the results in a useable way (Matheys, et al., 2007). For the use of this study, the functional unit of per kWh was chosen. The functional kWh is defined as the total amount of energy given over a lifetime (per kg) and is calculated using

$$\text{Functional energy density} = \text{energy density} \times \text{number of discharges over lifetime}$$

$$15 \text{ Wh kg}^{-1} \times 1750 \text{ cycles} = 26.25 \text{ kWh kg}^{-1}$$

Converting this to kWh/kg and taking the inverse gives 0.038 kg per functional kWh. From values given in (Holland, et al., 2018) for the electrode mass, the mass per kWh is determined as ~0.026 kg for the negative electrode and ~0.0118 kg for the positive electrode. Supporting material (such as electrolyte or battery casing) is scaled accordingly – with the cell mass assessed at ~7 kg. It is important to note that given the Al-ion cell's high power density (300 W kg⁻¹) it has applications similar to a supercapacitor (Smith, et al., 2020), and so a second functional unit defined as functional kW will also be assessed when comparing the environmental impacts to supercapacitors in section 3.2, to give a more realistic understanding of the impacts.

$$\text{Functional power density} = \text{power density} \times \text{number of discharges over lifetime}$$

$$300 \text{ W kg}^{-1} \times 1750 \text{ cycles} = 525 \text{ kW kg}^{-1}$$

And taking the inverse gives 0.002 kg kW⁻¹. Therefore, the results presented per kWh can be multiplied by a factor of 0.053 to provide the impacts per kW.

3. Results and discussion

Using OpenLCA and the EUEF midpoint analysis, the impacts of production were assessed over 19 impact categories, grouped as (a) acidification, (b) carcinogenic properties, (c) climate impact, (d) land usage, (e) ozone impact and (f) energy resource:

- (a) Acidification of water, reported as an increase in Mole of H⁺ eq., reduces the amount of carbonate available for sea life, and affects their environment. Most notably it can limit growth of corals and plankton which serve as vast ecosystems for many other marine life (Doney, et al., 2009, Bach, et al., 2016). Ecotoxicity of freshwater measured in Comparative Toxic Units ecotoxicity (CTUe), attempts to understand the overall pollution to freshwater, from air, land run-off (such as pesticides) and direct chemical release into the water (Otte, 2016). Eutrophication refers to the increase of nutrients to water, such that algae and other organisms thrive on the surface, blocking sun and depriving oxygen to those living below the surface. Due to the processes by which eutrophication takes place in different bodies of

water, it is measured in kg P eq. in freshwater, kg N eq. for marine water, and as an increase in Mole of N eq. for terrestrial water.

- (b) Cancer causing human health effects, measured in Comparative Toxic Unit for human (CTUh), provides the increased risk of morbidity from cancer for the entire human population, given the chemicals emitted during the production process. Similarly, non-cancer-causing human health effects are also measured in CTUh and summarise other potential hazards. Ionising radiation is assessed in a separate category, given as kBq U₂₃₅ eq. released. The release of respiratory inorganics, in the form of particles less than 2.5µm in diameter, can also cause lung disease and irritation, and are measured as kg PM2.5 eq.
- (c) Climate change impact is given as kg CO₂ eq. added to the atmosphere. This category is then subdivided into impacts from biogenic sources (such as burning wood or other bio-fuels), fossil sources (such as petrol or other crude oil products) and through land use change (such as from deforestation and the reduction of carbon sinks).
- (d) Land use is given in eco-points, Pt, which takes into account the use of the land, the area and the amount of time for which the land is in use – for example, grazing an animal may take a different amount of time than growing crops for the same area.
- (e) O-zone contribution is split into two categories, Ozone depletion, given in kg CFC eq. (kg chlorofluorocarbons eq.) which is in terms of the upper atmosphere. O-zone formation is also assessed, as at a local level this impacts human health, in kg non-methane volatile organic compounds eq. (kg NMVOC eq.).
- (f) Resource use is quantified as an energy in MJ. The use of minerals and metals (such as through mining) is measured in kg Sb eq. The use of water is assessed in m³ water.

3.1. Al-ion battery per kWh

Using OpenLCA and the EUEF midpoint analysis, the impacts of production were assessed per functional kWh. The total impact in a variety of categories was calculated. Table 2 shows the absolute values of each category per functional kWh, whereas Table 3 shows the results normalised and weighted to the product environmental footprint (PEF) suggested values (Potocnik, 2013) – which aim to quantify the impacts so that they can be compared to each other. The top 5 impact categories- taken as the categories with the highest normalised values, obtained from the data obtained in Table 3 are analysed further to identify their main contributors. These are, respiratory inorganics (6.74×10^{-7} kg PM2.5 eq.), resource use – energy carriers ($4.10 \times 10^{+1}$ MJ) and minerals and metals (9.18×10^{-5} kg Sb eq.), climate change ($2.95 \times 10^{+0}$ kg CO₂ eq. overall) and acidification of water (1.76×10^{-2} Mole of H⁺ eq.). These are presented graphically in Figure 8. The percentage impact contribution is provided for the production of: AlCl₃, copper battery casing, electrode substrate, KCl and ‘other’. The category ‘other’ includes all other processes assessed during the impact assessment.

Table 2 Impact assessment per functional kWh

Impact category	Value
Acidification terrestrial and freshwater [Mole of H ⁺ eq.]	1.76×10^{-2}
Cancer human health effects [CTUh]	6.62×10^{-8}
Climate Change [kg CO ₂ eq.]	$2.95 \times 10^{+0}$
Climate Change (biogenic) [kg CO ₂ eq.]	2.46×10^{-3}

Climate Change (fossil) [kg CO ₂ eq.]	2.95× 10 ⁺⁰
Climate Change (land use change) [kg CO ₂ eq.]	1.83× 10 ⁻³
Ecotoxicity freshwater [CTUe]	1.91× 10 ⁺⁰
Eutrophication freshwater [kg P eq.]	8.92× 10 ⁻⁵
Eutrophication marine [kg N eq.]	4.11× 10 ⁻³
Eutrophication terrestrial [Mole of N eq.]	4.45× 10 ⁻²
Ionising radiation - human health [kBq U ₂₃₅ eq.]	1.87× 10 ⁻¹
Land Use [Pt]	5.15× 10 ⁺⁰
Non-cancer human health effects [CTUh]	5.73× 10 ⁻⁷
Ozone depletion [kg CFC-11 eq.]	4.50× 10 ⁻⁷
Photochemical ozone formation - human health [kg NMVOC eq.]	1.08× 10 ⁻²
Resource use, energy carriers [MJ]	4.10× 10 ⁺¹
Resource use, mineral and metals [kg Sb eq.]	9.18× 10 ⁻⁵
Respiratory inorganics[kg PM2.5 eq.]	6.74× 10 ⁻⁷
Water scarcity [m ³ world equiv.]	7.50× 10 ⁻¹

Table 3 Normalised and weighted impact assessment per function kWh, with highest impact results in bold

Impact Category	Value
Acidification terrestrial and freshwater	2.1 × 10⁻⁵
Climate Change	8.44 × 10⁻⁵
Eutrophication freshwater	1.03 × 10 ⁻⁶
Eutrophication marine	4.52 × 10 ⁻⁶
Eutrophication terrestrial	9.81 × 10 ⁻⁶
Ionising radiation - human health	2.38 × 10 ⁻⁶
Land Use	3.25 × 10 ⁻⁷
Ozone depletion	1.30 × 10 ⁻⁶
Photochemical ozone formation - human health	1.36 × 10 ⁻⁵
Resource use, energy carriers	5.59 × 10⁻⁵
Resource use, mineral and metals	1.28 × 10⁻⁴
Respiratory inorganics	1.01 × 10⁻⁴
Water scarcity	5.88 × 10 ⁻⁶

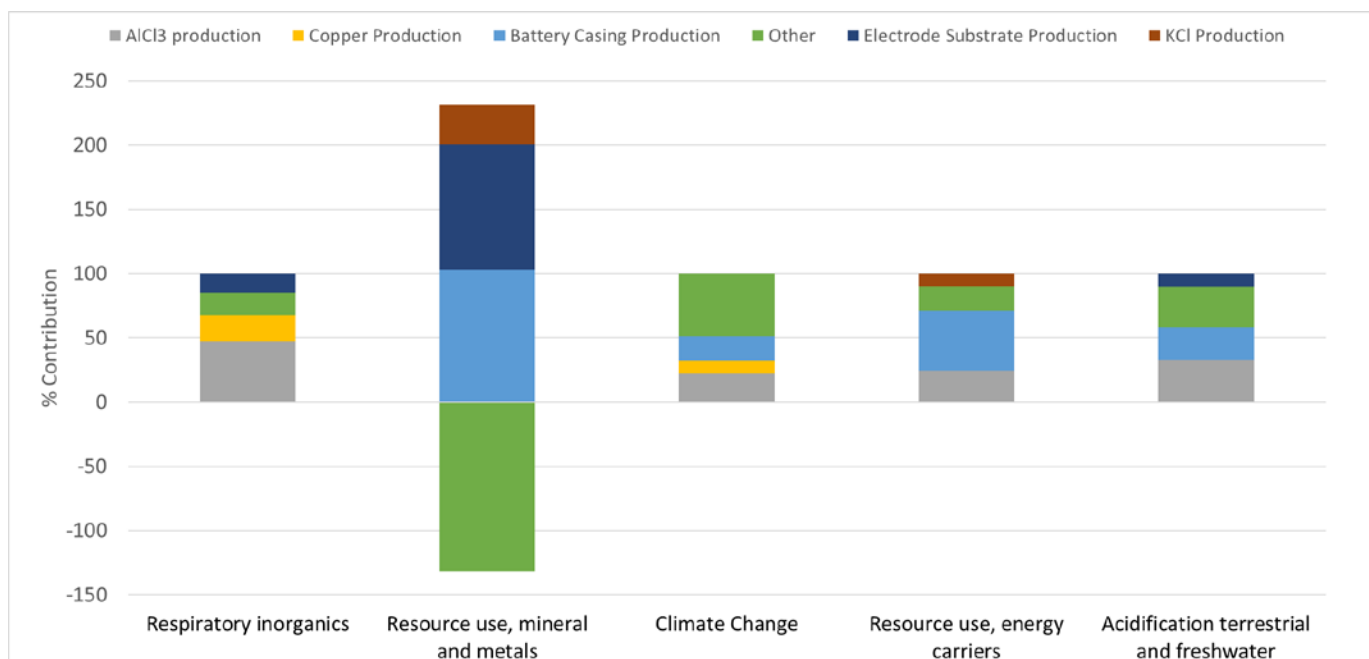


Figure 8 Top five impact categories with their main contributors

Figure 8 shows that the battery casing productions – which includes the mining of hydrocarbons through to the production of the plastic granulates – appears as a contributor to the main impacts. It is again worth mentioning that the assumption of casing mass was based off an Li-ion battery, and when using a lower mass for the casing, the impacts of this are reduced. Plastic is also highly recyclable, thus changing the input of the battery casing to a higher percentage recycled plastic would again reduce the impacts of this component.

In terms of the copper contribution for the current collector, this could be reduced by looking into recycling methods at end of life (EoL), for Pb-acid batteries the recycling/reuse accounts for -21% of the overall impact (Liu, et al., 2015). However, copper is not the only current collector option, there are many polymer or other metal foils which could be investigated for use in this cell. The choice for this component within the software was ‘copper sheet’, whereas for the production of CuHCF, ‘copper mix’ was used as they have different production methods (see S1 for component breakdown). It is important to note, that the negative ‘other’ within the ‘Resource use; minerals and metals’ category is due to the CuHCF copper production, as it is assumed that for the CuHCF production 40% of the copper was from scrap or recycled sources. These assumptions can make a large difference in the outcome of the LCA, and therefore the recyclability of copper in all aspects of the cell will be assessed in future work.

The impacts from the electrolyte cannot be reduced through a substitution, however recycling at EoL will most likely play a role in reducing the overall impact. In terms of the aluminium, it has been shown that recycled Al uses 10% of the energy needed for primary production (Butterwick and Smith, 1986, Agency, 2009).

It is important to bear in mind that there were many assumptions made within this analysis. The key difficulties with this task were in finding the appropriate production methods for branded products such as Nafion, as well as the Electrode substrate, and thus a more general descriptor was used – which may not have taken into account the key production processes and waste produced. Many assumptions were made on transport distances based on the locations of productive mines and

manufacturing plants around the world – however these were in line with those recommended (and therefore used) in (Siret, 2018).

3.2. Comparison to supercapacitors

To compare the values with those produced in (Cossutta, et al., 2020) resources needed in order to manufacture the batteries were added – along with a charger, to match the analysis. These values were taken from (Siret, 2018) as they had not been assessed for the initial impact assessment. Key additions to this analysis were electricity (0.82 MJ) and water (0.48 kg) used in the manufacturing process. A full breakdown of components and the relevant datasets used can be found in S1. As mentioned previously, given the Al-ion cell's tendency to perform like a supercapacitor, potential commercial applications could complement or even replace supercapacitor roles in the future. The Al-ion cell is already seen as a cheaper alternative to expensive supercapacitors, and therefore it is important to evaluate the environmental impacts as well. (Salgado Delgado, 2019, Holland, 2018, Smith, et al., 2020, Pan, et al., 2019). The values presented in Table 4 are calculated per functional kW over the lifetime of the assessed supercapacitors described in (Cossutta, et al., 2020) for a cradle-to-gate scenario. This FU was calculated as shown in section 2.3.

When compared with the Graphene (rGO) and Activated carbon (AC) supercapacitors in Table 5, Al-ion has fewer impacts per kW in all categories. A breakdown of climate change contributions isn't provided in (Cossutta, et al., 2020), however, in total, Al-ion batteries produce an order of magnitude less kg CO₂ eq. per kW ($\sim 10^{-1}$ for Al-ion and $\sim 10^0$ for both supercapacitors). Electrode manufacture, and electricity use are reported as the key contributors to this category (Cossutta, et al., 2020). The resource use (energy carriers) for the two supercapacitors, is an order of magnitude higher than that of Al-ion - $\sim 10^{+1}$ and 10^{+0} MJ per kW respectively. The production techniques involved for manufacturing these supercapacitors, overall, are reported as more energy intense than for the battery. This may be due to the more complex manufacturing processes for the advanced materials used in the supercapacitors.

Discussion in (Cossutta, et al., 2020), mentions uncertainty in techniques for measuring and understanding the emission of nanoparticles in the production of advanced materials for supercapacitors, and therefore it was not fully included in the LCA. For the Al-ion battery, the TiO₂ electrode uses anatase nanopowder – an item not found in the datasets used, and so the 'nano' aspect of the material in the Al-ion LCA was also not fully accounted for. This leads to uncertainty on the exact impact of respiratory inorganics, as a method for accounting for nanomaterial release has not yet been formalised (Salieri, et al., 2018). Keeping this in mind – Al-ion still appears to emit four orders of magnitude less particulates than the supercapacitors in this analysis $\sim 10^{-8}$ and $\sim 10^{-4}$ kg PM2.5 eq. respectively.

The key contributor to this category for the supercapacitors is the production of electrodes (Cossutta, et al., 2020). While not fully explored in the paper – the use of N-Methylpyrrolidone (NMP) is common in supercapacitor manufacture. It is a solvent used in the production of electrodes, and is linked with a high impact in the respiratory particulate category (Arunkumar and Amit, 2017). Isopropanol is used as a solvent in the production of the Al-ion electrodes which has a negligible contribution to this impact category. More research into the use of appropriate solvents when scaling up the production is needed to fully understand the choice and impact on respiratory inorganics.

The Al-ion battery has an order of magnitude more impact on O-zone depletion - $\sim 10^{-8}$ kg CFC-11 eq. for Al-ion compared to $\sim 10^{-9}$ kg CFC-11 eq. for the supercapacitors. The main contributor to this is the electrode manufacture for both supercapacitors (Cossutta, et al., 2020), though the main details are not fully explored. A key contributor to this category for Al-ion is the production of tetrafluoroethylene, a material modelled in the production of Nafion – the binder for the electrode ink. This may refer to the estimates made when modelling Nafion, however it may also be useful to investigate alternate binder materials for future battery designs. When normalised and weighted for impact, however, overall O-zone depletion has negligible impact.

The water use in producing Al-ion batteries is high compared to the supercapacitors (for rGO 1.82×10^{-2} m³, for AC 8.45×10^{-3} m³, and for Al-ion 2.48×10^{-1} m³). The main contribution to this category is the water added to model production, taken from (Siret, 2018), and may not be completely valid. Further investigation into the production method of the Al-ion cells is needed to get a clearer picture.

Table 4 Comparison with Graphene (rGO) and Activated carbon (AC) supercapacitors per kW with this work. Values calculated from (Cossutta, et al., 2020) supplementary information.

Impact category	rGO/kW (Cossutta, et al., 2020)	AC/kW (Cossutta, et al., 2020)	Al-ion/kW (this work)
Acidification terrestrial and freshwater [Mole of H+ eq.]	1.08×10^{-2}	5.43×10^{-3}	1.67×10^{-3}
Cancer human health effects [CTUh]	5.19×10^{-9}	1.75×10^{-9}	5.73×10^{-9}
Climate Change [kg CO ₂ eq.]	$2.53 \times 10^{+0}$	$1.05 \times 10^{+0}$	2.61×10^{-1}
Climate Change (biogenic) [kg CO ₂ eq.]	Not provided		3.89×10^{-4}
Climate Change (fossil) [kg CO ₂ eq.]			2.61×10^{-1}
Climate Change (land use change) [kg CO ₂ eq.]			1.68×10^{-4}
Ecotoxicity freshwater [CTUe]	1.39×10^{-1}	4.74×10^{-2}	1.57×10^{-1}
Eutrophication freshwater [kg P eq.]	4.98×10^{-6}	1.23×10^{-6}	2.81×10^{-5}
Eutrophication marine [kg N eq.]	Not provided		3.48×10^{-4}
Eutrophication terrestrial [Mole of N eq.]	1.73×10^{-2}	8.38×10^{-3}	3.68×10^{-3}
Ionising radiation - human health [kBq U ₂₃₅ eq.]	6.56×10^{-1}	1.68×10^{-1}	3.53×10^{-2}
Land Use [Pt]	Not provided		5.39×10^{-1}
Non-cancer human health effects [CTUh]	8.09×10^{-8}	3.33×10^{-8}	6.79×10^{-8}
Ozone depletion [kg CFC-11 eq.]	1.01×10^{-9}	1.07×10^{-9}	7.01×10^{-8}
Photochemical ozone formation - human health [kg NMVOC eq.]	4.96×10^{-3}	2.39×10^{-3}	9.01×10^{-4}
Resource use, energy carriers [MJ]	$5.61 \times 10^{+1}$	$2.33 \times 10^{+1}$	$4.37 \times 10^{+0}$
Resource use, mineral and metals [kg Sb eq.]	3.04×10^{-5}	8.83×10^{-6}	1.04×10^{-5}
Respiratory inorganics [kg PM _{2.5} eq.]	5.87×10^{-4}	3.28×10^{-4}	4.52×10^{-8}
Water scarcity [m ³ world equiv.]	1.82×10^{-2}	8.45×10^{-3}	2.48×10^{-1}

4. Conclusions

This work presents the first life-cycle assessment for an Al-ion aqueous electrolyte cell. The production of the salt, AlCl_3 , as well as the plastic battery casing, contribute highly to the environmental impacts (22% and 18% respectively of the kg CO_2 eq. emitted). However, this assessment did not include recycling, which may reduce impact of these processes.

Compared to supercapacitors, the cell had significantly less impact in terms of energy resource (~81% reduction), respiratory inorganics (~100% reduction), and climate change (~75% reduction), with comparable values for the other impact categories per kW. This presents an argument for the development of Al-ion aqueous technology as a sustainable energy storage device when comparing to supercapacitors.

Aqueous Al-ion cells are currently pre-commercial systems. As such, this study can be used in synergistic development for the battery, which minimises environmental impact of materials and design choices in its future development. For example, the use of isopropanol over NMP as a solvent has reduced particulate impact, but the use of the Nafion binder increases the contribution to O-zone depletion, and other binders may be interesting to study.

Furthermore, increasing the capacity of the cell will require either increasing the quantity of active material per cell or reducing the percentage of non-active material. For example, identifying materials with reduced mass for the electrode substrates to replace the carbon-polymer currently used can be assessed from an environmental perspective against the inclusion of 3D active material scaffolds for increasing the percentage of active material per cell. These activities can now be run alongside the LCA to identify a balance between environmental impact and device performance.

Further work is also needed to expand the results displayed in this work. This should comprise of an investigation into the use-phase and end-of-life, including re-use and recycling capabilities, to allow the full life cycle assessment to be made and compared to other energy storage options.

Conflict of Interest

All financial, commercial or other relationships that might be perceived by the academic community as representing a potential conflict of interest must be disclosed. If no such relationship exists, authors will be asked to confirm the following statement:

The authors declare that the research was conducted in the absence of any commercial or financial relationships that could be construed as a potential conflict of interest.

Author Contributions

NM- research, analysis, writing

RGAW – reviewing and writing

AJC – reviewing

5. Funding

This work was funded by UKRI under an STFC Studentship and the EPSRC Faraday Training Grant EP/S514901/1

References

- G. A. Elia, K. V. Kravchyk, M. V. Kovalenko, J. Chacón, A. Holland and R. G. A. Wills. An overview and prospective on Al and Al-ion battery technologies. *Journal of Power Sources*. (2021), 481. 228870. <https://doi.org/10.1016/j.jpowsour.2020.228870>
- L. A. Ellingsen, A. Holland, J.-F. Drillet, W. Peters, M. Eckert, C. Concepcion, O. Ruiz, J.-F. Colin, E. Knipping, Q. Pan, R. G. A. Wills and G. Majeau-Bettez. Environmental Screening of Electrode Materials for a Rechargeable Aluminum Battery with an AlCl₃/EMIMCl Electrolyte. *Materials*. (2018), 11. 10.3390/ma11060936
- M. U. Salgado Delgado, L; Ellingsen, L-W; Pan, Q, Hammer Strømman, A. Comparative Life Cycle Assessment of a Novel Al-Ion and a Li-Ion Battery for Stationary Applications. *Materials*. (2019), 12. <https://doi.org/10.3390/ma12193270>
- A. Holland, R. D. McKerracher, A. Cruden and R. G. A. Wills. An aluminium battery operating with an aqueous electrolyte. *Journal of Applied Electrochemistry*. (2018), 48. 243-250. 10.1007/s10800-018-1154-x
- M. Conte, A. Genovese, F. Ortenzi and F. Vellucci. Hybrid battery-supercapacitor storage for an electric forklift: a life-cycle cost assessment. *Journal of Applied Electrochemistry*. (2014), 44.
- M. Cossutta, V. Vretenar, T. A. Centeno, P. Kotrusz, J. McKechnie and S. J. Pickering. A comparative life cycle assessment of graphene and activated carbon in a supercapacitor application. *Journal of Cleaner Production*. (2020), 242. 118468. <https://doi.org/10.1016/j.jclepro.2019.118468>
- C. Siret, Tytgat, J., Ebert, T., Mistry, M. (2018). Product Environmental Footprint Category Rules for High Specific Energy Rechargeable Batteries for Mobile Applications.
- J. Potocnik. Commission Recommendation of 9 April 2013 on the use of common methods to measure and communicate the life cycle environmental performance of products and organisations Text with EEA relevance. *Official Journal of the European Union*. (2013), 56. 10.3000/19770677.L_2013.124.eng
- A. Holland. (2018). Development and characterisation of an aqueous aluminium-ion battery. PhD Thesis. University of Southampton

A. Ciroth. ICT for environment in life cycle applications openLCA — A new open source software for life cycle assessment. *The International Journal of Life Cycle Assessment*. (2007), 12. 209. 10.1065/lca2007.06.337

B. Steubing, G. Wernet, J. Reinhard, C. Bauer and E. Moreno-Ruiz. The ecoinvent database version 3 (part II): analyzing LCA results and comparison to version 2. *The International Journal of Life Cycle Assessment*. (2016), 21. 1269-1281. 10.1007/s11367-016-1109-6

A. Thinkstep. (2012). GaBi Software System and database for Life Cycle Engineering

K. A. Mauritz and R. B. Moore. State of Understanding of Nafion. *Chemical Reviews*. (2004), 104. 4535-4586. 10.1021/cr0207123

Sigracell. (2016). Speciality Graphites for Energy Storage.

J.-Y. Choi, D. J. Lee, Y. M. Lee, Y.-G. Lee, K. M. Kim, J.-K. Park and K. Y. Cho. Silicon Nanofibrils on a Flexible Current Collector for Bendable Lithium-Ion Battery Anodes. *Advanced Functional Materials*. (2013), 23. 2108-2114. <https://doi.org/10.1002/adfm.201202458>

A. D. Ballantyne, J. P. Hallett, D. J. Riley, N. Shah and D. J. Payne. Lead acid battery recycling for the twenty-first century. *Royal Society Open Science*. (2018), 5. 171368. 10.1098/rsos.171368

W. Liu, J. Sang, L. Chen, J. Tian, H. Zhang and G. Olvera Palma. Life cycle assessment of lead-acid batteries used in electric bicycles in China. *Journal of Cleaner Production*. (2015), 108. 1149-1156. <https://doi.org/10.1016/j.jclepro.2015.07.026>

J. F. Peters and M. Weil. Providing a common base for life cycle assessments of Li-Ion batteries. *Journal of Cleaner Production*. (2018), 171. 704-713. <https://doi.org/10.1016/j.jclepro.2017.10.016>

H. C. Kim, T. J. Wallington, R. Arsenault, C. Bae, S. Ahn and J. Lee. Cradle-to-Gate Emissions from a Commercial Electric Vehicle Li-Ion Battery: A Comparative Analysis. *Environmental Science & Technology*. (2016), 50. 7715-7722. 10.1021/acs.est.6b00830

U.S. Geological Survey, Mineral Commodity Summaries. (2020). 200.

J. Matheys, W. Van Autenboer, J.-M. Timmermans, J. Van Mierlo, P. Van den Bossche and G. Maggetto. Influence of functional unit on the life cycle assessment of traction batteries. *The International Journal of Life Cycle Assessment*. (2007), 12. 191. 10.1065/lca2007.04.322

B. D. Smith, R. G. A. Wills and A. J. Cruden. Aqueous Al-ion cells and supercapacitors — A comparison. *Energy Reports*. (2020), 6. 166-173. <https://doi.org/10.1016/j.egy.2020.03.021>

S. C. Doney, V. J. Fabry, R. A. Feely and J. A. Kleypas. Ocean Acidification: The Other CO₂ Problem. *Annual Review of Marine Science*. (2009), 1. 169-192.
10.1146/annurev.marine.010908.163834

V. Bach, F. Möller, N. Finogenova, Y. Emara and M. Finkbeiner. (2016). Characterization model to assess ocean acidification within life cycle assessment. 21. 1463-1472.10.1007/s11367-016-1121-x

N. Otte. (2016). Freshwater ecotoxicity as an impact category in life cycle assessment.

L. Butterwick and G. D. W. Smith. Aluminium recovery from consumer waste—I. Technology review. *Conservation & Recycling*. (1986), 9. 281-292. [https://doi.org/10.1016/0361-3658\(86\)90018-4](https://doi.org/10.1016/0361-3658(86)90018-4)

I. E. Agency. (2009). Energy Technology Transitions for Industry.
doi:<https://doi.org/10.1787/9789264068612-en>

L. Van Oers, A. De Koning, J. B. Guinée and G. Huppes. Abiotic resource depletion in LCA. Road and Hydraulic Engineering Institute, Ministry of Transport and Water, Amsterdam. (2002),

W. Pan, Y. Wang, Y. Zhang, H. Y. H. Kwok, M. Wu, X. Zhao and D. Y. C. Leung. A low-cost and dendrite-free rechargeable aluminium-ion battery with superior performance. *Journal of Materials Chemistry A*. (2019), 7. 17420-17425. 10.1039/C9TA05207K

B. Salieri, D. A. Turner, B. Nowack and R. Hischier. Life cycle assessment of manufactured nanomaterials: Where are we? *NanoImpact*. (2018), 10. 108-120.
<https://doi.org/10.1016/j.impact.2017.12.003>

M. Arunkumar and P. Amit. Importance of Electrode Preparation Methodologies in Supercapacitor Applications. *ACS Omega*. (2017), 2. 8039-8050. 10.1021/acsomega.7b01275